Statistics of incremental averages of passive scalar fluctuations

Colin R. Meyer
Department of Earth Sciences, University of Oregon, Eugene, Oregon 97403, USA

Laurent Mydlarski*
Department of Mechanical Engineering, McGill University, Montréal, Québec, Canada, H3A 0C3

Luminita Danaila
CORIA, University of Rouen Normandy, 76801 Saint Etienne du Rouvray, France

(Received 25 November 2017; published 7 September 2018)

Whereas statistical moments of differences of turbulent quantities measured over a given separation (viz., structure functions) have been extensively studied, statistics of incremental sums (or equivalently averages, e.g., $\Sigma\theta \equiv [\theta(x+r)+\theta(x)]/2$) of the same quantities have only been the subject of recent research. The present work investigates incremental averages of a turbulent passive scalar (temperature), measured in nearly homogeneous, and isotropic (passive and active), grid-generated turbulence, for turbulent Reynolds numbers in the range $94 \leqslant R_\lambda(\equiv u_{\rm rms}\lambda/\nu) \leqslant 582$. The scalar field is generated by the action of the turbulent velocity field against an imposed mean temperature gradient. Following the approach of Mouri and Hori [Phys. Fluids **22**, 115110 (2010)] for the velocity field, we examine statistics of incremental averages of the passive scalar field as a function of separation (viz., incremental average structure functions) for different Reynolds numbers, comparing them with both the results of Mouri and Hori, as well as the corresponding incremental average structure functions for the velocity field for the flows studied herein. While the statistics of $\Sigma\theta$ are *primarily* large-scale quantities, and would therefore be expected to be flow dependent, they exhibit certain similarities to the statistics of incremental averages of velocity (Σu_α), measured both in the flow under consideration as well as the different classes of flows studied by Mouri and Hori. Finally, we derive a scale-dependent evolution equation for the incremental average of the scalar field fluctuations, $\Sigma\theta$. We discuss its relationship to Yaglom's four-thirds law for differences in passive scalar fluctuations and compare the results with the experimental data.

DOI: 10.1103/PhysRevFluids.3.094603

I. INTRODUCTION

In the years since Kolmogorov [1] published his theory of turbulent flows, there has been extensive experimental, numerical, and theoretical research on the small scales of turbulent velocity fields. Following the subsequent extension of Kolmogorov theory to passive scalar fields by Obukhov [2] and Corrsin [3], there has been significant research on the structure of turbulent passive scalar fields, although to a lesser extent than that on their hydrodynamic counterparts. Turbulent passive scalar fields, which at first glance might appear to be more straightforward than turbulent hydrodynamic fields (given the simpler nature of the advection-diffusion equation, as compared to the Navier-Stokes equations), are, in fact, quite distinct, exhibiting many unique behaviors. These include but are not limited to (i) the development of an inertial-convective subrange in homogeneous isotropic turbulence

*Corresponding author: laurent.mydlarski@mcgill.ca

TABLE I. Comparison of properties of the (traditional) incremental difference structure functions and those of incremental average structure functions, assuming statistical homogeneity in the x direction.

	Incremental difference structure functions	Incremental average structure functions
Definition	$\langle(\Delta\theta)^2\rangle \equiv \langle(\theta(x_i + r_i, t) - \theta(x_i, t))^n\rangle$	$\langle(\Sigma\theta)^2\rangle \equiv \left\langle\left[\frac{1}{2}(\theta(x_i + r_i) + \theta(x_i))\right]^n\right\rangle$
Relationship to the autocorrelation, $\rho_{\theta\theta}(r)$	$\frac{\langle(\Delta\theta)^2\rangle}{\langle\theta^2\rangle} = 2(1 - \rho_{\theta\theta}(r))$	$\frac{\langle(\Sigma\theta)^2\rangle}{\langle\theta^2\rangle} = \frac{1}{2}(1 + \rho_{\theta\theta}(r))$
Scaling	$\frac{\langle(\Delta\theta)^2\rangle}{\langle\theta^2\rangle} \sim Ar^{\gamma_\theta}$	$\frac{\langle(\Sigma\theta)^2\rangle}{\langle\theta^2\rangle} \sim 1 - Cr^{\gamma_\theta}$

(e.g., [4]) at Reynolds and Péclet numbers well below those that permit a substantial separation of scales (the latter being the fundamental underpinning of Kolmogorov theory), (ii) strong, local anisotropy of small-scale quantities in flows that are anisotropic at large scales (e.g., [5–7]), and (iii) higher levels of internal intermittency than observed in hydrodynamic fields [5,6]. For further details on turbulent passive scalar fields, the reader is referred to the reviews of Sreenivasan [8], Warhaft [9]. Shraiman and Siggia [10], and Dimotakis [11].

Given that Kolmogorov theory provides explicit predictions regarding their scaling, structure functions have played an important role and been the subject of numerous investigations of the small-scale statistics of turbulent fields. Small-scale statistics have been investigated by studying the structure functions, which are defined as the average of the difference between two values of a given quantity measured over a spatial (or temporal) interval, and raised to the power n. Using an arbitrary component of the turbulent velocity fluctuation (u_α) as an example, an nth-order structure function can be mathematically expressed as follows:

$$\left\langle\left(\Delta_{r_i} u_\alpha\right)^n\right\rangle \equiv \langle(u_\alpha(x_i + r_i, t) - u_\alpha(x_i, t))^n\rangle. \tag{1}$$

Structure functions provide information about the scaling of the small-scale turbulent fields. And although structure functions are sometimes claimed to be representative of the behavior of a given quantity at a scale r ($\equiv|r| = (r_i r_i)^{1/2}$), where the Einstein summation convention is only implied for roman indices, not greek ones, it is important to emphasize that structure functions also have contributions from scales smaller than r. To reinforce this point, note that the limit as r tends to zero of the second-order structure function of u_α is zero, whereas its limit as r tends to infinity is $2\langle u_\alpha^2\rangle$, which is four times the turbulent kinetic energy ($\frac{1}{2}\langle u_\alpha^2\rangle$) associated with the u_α component of velocity. Thus, a structure function contains contributions from all scales *less than or equal to* r, because the turbulent kinetic energy of a quantity has contributions from all scales. Recall that the turbulent kinetic energy can, after all, also be obtained from the integral of the power spectrum of a velocity fluctuation over all wave numbers.

Given the extensive attention that has been paid to structure functions, a different, but complementary, statistic has been proposed to further our understanding of turbulent flows: two-point incremental averages of turbulent quantities, defined as

$$\left\langle\left(\Sigma_{r_i} u_\alpha\right)^n\right\rangle \equiv \left\langle\left[\frac{u_\alpha(x_i + r_i) + u_\alpha(x_i)}{2}\right]^n\right\rangle. \tag{2}$$

When referring to incremental averages over a separation r, we use the phrase incremental average structure functions (IASFs), which are to be contrasted with traditional structure functions—like those defined by Eq. (1)—which we refer to as incremental difference structure functions (IDSFs). The present work studies statistics of IASFs, with an emphasis on those of passive scalar fields. A brief comparison of the properties of IDSFs and IASFs (written for passive scalar fields) is given in Table I. Note that from here on in, the subscript in "r_i" is omitted (i.e., "r"), for the sake of concision.

Previous researchers have studied statistics of incremental averages, with Sreenivasan and Dhruva [12] being among the earliest to do so. Using atmospheric velocity measurements, they found the probability density function (PDF) of Σu to be nearly identical to the PDF of u. They also studied the expectations of incremental difference structure functions, conditioned on the velocity at the midpoint of an interval, which they noted gave the same results as conditioning on the incremental average velocity. Tatsumi and co-workers [13–15] theoretically studied the velocity sum PDF in homogeneous, isotropic turbulence using the cross-independence closure hypothesis. Statistics of incremental averages are also especially relevant to the (unresolved) question of whether large- and small-scale statistics of turbulent fields are statistically independent (e.g., [16]). This question has been recently studied by Hosokawa [17], Kholmyansky and Tsinober [18], and Blum *et al.* [19]. Moreover, the energy transfer between two-point averages of a velocity field and its respective two-point differences was studied by Germano [20], who showed that the transfer can be viewed as being produced by the subgrid stress associated with the two-point average, or related to the classical, second-order IDSF. Finally, of particular interest to the present work is the work of Mouri and Hori [21], who extensively studied (longitudinal) incremental averages of the longitudinal and transverse velocity fluctuations ($\langle(\Sigma_r u)^n\rangle$ and $\langle(\Sigma_r v)^n\rangle$, respectively) in grid turbulence, a turbulent boundary layer, and a turbulent jet. Their work will serve as a reference for the results presented herein. In summary, given their relevance to both fundamental and applied issues in the study of turbulence, statistics of incremental averages merit further study.

To further contrast IDSFs and IASFs, we remark that a power-law scaling range (i.e., $\propto r^n$) is not expected to be (explicitly) observed in the statistics of incremental averages. However, in the limit of high Reynolds and Péclet numbers, the second-order incremental average structure function can be expected to scale as $1 - Cr^{\gamma_\theta}$, where γ_θ is the inertial-convective range scaling exponent of the second-order incremental difference structure function, $\langle(\Delta\theta)^2\rangle$. This result stems from an easily derivable relationship between the second-order IDSF and the second-order IASF [21]:

$$\frac{\langle(\Sigma\theta)^2\rangle}{\langle\theta^2\rangle} = 1 - \frac{\langle(\Delta\theta)^2\rangle}{4\langle\theta^2\rangle}, \tag{3}$$

or, equivalently,

$$\langle(\Sigma\theta)^2\rangle + \tfrac{1}{4}\langle(\Delta\theta)^2\rangle = \langle\theta^2\rangle, \tag{4}$$

which can equivalently be derived from the relationships in Table I by eliminating $\rho_{\theta\theta}$ and assuming statistical homogeneity in the x direction—an assumption that is relaxed in Sec. III.

From Eq. (4), it can be concluded that motions at scales greater than or equal to r (as hypothesized by Mouri and Hori [21]) contribute to IASFs because (i) $\langle\theta^2\rangle$ has contributions from all scales ($0 < r < \infty$) and (ii) $\langle(\Delta\theta)^2\rangle$ is determined by motions at scales less than or equal to r, as previously noted. This conclusion is directly related to the previous arguments pertaining to the scales on which IDSFs depend. Moreover, it explains the following result obtained by Hosokawa [17] for turbulence that is homogeneous in the x direction:

$$\langle(\Delta u)(\Sigma u)^2\rangle = -\tfrac{1}{12}\langle(\Delta u)^3\rangle, \tag{5}$$

which, in the inertial subrange, can be rewritten as

$$\langle(\Delta u)(\Sigma u)^2\rangle = \tfrac{1}{15}\langle\epsilon\rangle r \tag{6}$$

without an invocation of a correlation between large- and small-scale motions, as proposed by Hosokawa [17], and where ϵ denotes the dissipation rate of turbulent kinetic energy, $\frac{\nu}{2}(\partial u_i/\partial x_j + \partial u_j/\partial x_i)^2$, where ν is the fluid kinematic viscosity. Rather, the nonzero correlation between Δu and $(\Sigma u)^2$ arises from the fact that both have nonzero contributions at scale r.

To conclude this section we state the main objectives of the present work, which are to (i) provide the first measurements (to our knowledge) of incremental averages of a turbulent scalar field, (ii) provide further insight on the structure of turbulent passive scalar fields by means of the aforementioned measurements, and (iii) theoretically and experimentally investigate the relationship between incremental averages of a turbulent scalar field and the velocity field that advects it. To these ends, we study passive scalar fields generated by a mean temperature gradient in grid turbulence (generated by both passive and active grids) over the Reynolds number range $94 \leqslant R_\lambda \leqslant 582$. In addition, we present experimental measurements of incremental averages of the longitudinal and transverse velocity fields, and compare them with those of the scalar field. The remainder of this paper is organized as follows. The apparatus is described in Sec. II. The results (of both the scalar and velocity fields) are presented and discussed in Sec. III. Conclusions follow in Sec. IV.

II. APPARATUS

The measurements presented herein were made in the 0.91 m × 0.91 m × 9.1 m low-speed, low-background-turbulence wind tunnel in the Sibley School of Mechanical and Aerospace Engineering at Cornell University. The experiments and apparatus have been described in Refs. [6,22]. Therefore, the discussion herein of the apparatus is relatively brief.

The flow is homogeneous, quasi-isotropic, grid-generated turbulence. One set of measurements employed a passive grid with a mesh length (M) of 10.16 cm (4 in.). Larger Reynolds (and Péclet) numbers were obtained by use of an active grid [23–25]. The mean temperature gradient is generated by a set of differentially heated ribbons placed in the wind tunnel plenum chamber (see [6,26,27]). The mean flow is in the x direction while the mean scalar gradient is in the y direction. Both the velocity and temperature fields are statistically homogeneous in the z direction.

The longitudinal and transverse components of velocity were measured by a TSI 1241 X-wire probe with 3.05-μm-diameter tungsten wires that were operated using Dantec 55M01 constant-temperature anemometers. The length-to-diameter ratio of each wire was approximately 200 and the interwire spacing was 0.5 mm. The turbulent temperature field was measured by cold-wire thermometry in conjunction with a TSI 1210 probe to which 0.63-μm-diameter platinum core Wollaston wire was soldered. The cold-wire was located 0.5 mm from the X-wire and its length-to-diameter ratio varied from 500 to 650, depending on the flow. The hot-wire signals were calibrated using a modified King's law with temperature-dependent coefficients [28] to account for the fluctuating temperature of the flow. Time series of the two components of velocity and temperature were high- and low-pass filtered, sampled at twice the Kolmogorov frequency, and digitized using a 12-bit analog-to-digital converter. Spatial separations (used in the definition of the incremental average) are all in the longitudinal (x) direction and were obtained using Taylor's hypothesis. The associated flow parameters are outlined in Table II. For more details on the flows, the reader is referred to [6,22].

III. RESULTS AND DISCUSSION

The presentation of the results is subdivided into four sections. We begin in Sec. III A with a derivation of an analog to Hosokawa's equation [Eq. (6)] for the passive scalar field. In Sec. III B, we present incremental average structure functions for the scalar field, and compare them with those of the velocity field. In Sec. III C, we describe the probability density functions and conditional expectations of incremental averages. Finally, we present a modified Yaglom's equation, written for incremental sums (instead of incremental differences) in Sec. III D.

A. Passive scalar analog of Hosokawa's equation

Before presenting an equation for the passive scalar field that is analogous to Hosokawa's equation [Eq. (6)] for the velocity field, a more detailed discussion of the derivation of the latter equation is in order. A general version of Hosokawa's equation, which does not invoke the assumption of homogeneity of the field under consideration, can be derived. By (i) adding the (algebraic) expansions of $\langle(\Delta u)^3\rangle$ and $\langle(\Delta u)(\Sigma u)^2\rangle$, (ii) simplifying the expression by removing the terms that cancel out, and (iii) regrouping terms, one obtains the following expression:

$$\langle(\Delta u)^3\rangle + 4\langle(\Delta u)(\Sigma u)^2\rangle = 4\langle(\Delta u)\Sigma(u^2)\rangle, \tag{7}$$

TABLE II. Flow parameters.

Grid Grid Mode	Passive n/a	Active Synchronous	Active Random	Active Random
M (cm)	10.16	11.43	11.43	11.43
x/M	70	62	62	62
ν ($\mathrm{m^2\,s^{-1}}$)	15.7×10^{-6}	16.0×10^{-6}	16.0×10^{-6}	16.0×10^{-6}
β (°C/m)	7.4	15.6	2.7	3.6
κ ($\mathrm{m^2\,s^{-1}}$)	22.0×10^{-6}	22.5×10^{-6}	22.5×10^{-6}	22.5×10^{-6}
U ($\mathrm{m\,s^{-1}}$)	6.17	5.43	3.32	7.00
$\langle u^2\rangle$ ($\mathrm{m^2\,s^{-2}}$)	0.0219	0.121	0.0911	0.583
$\langle\theta^2\rangle$ (°C^2)	0.147	3.65	0.800	1.07
$\langle\epsilon\rangle\left(=15\nu\int_0^\infty k_1^2F_{11}(k_1)dk_1\right)$ ($\mathrm{m^2\,s^{-3}}$)	0.0521	0.278	0.0833	0.940
$\langle\epsilon_\theta\rangle$ $\left(=3\frac{\kappa}{U^2}\left\langle\left(\frac{d\theta}{dt}\right)^2\right\rangle\right)$ (°C^2 s^{-1})	0.126	3.73	0.353	0.768
R_λ $(=\langle u^2\rangle[15/(\nu\epsilon)]^{1/2})$	94	222	306	582
R_ℓ $(=\langle u^2\rangle^{1/2}\ell/\nu)$	528	2960	5600	20300
η $(=(\nu^3/\epsilon)^{1/4})$ (m)	5.2×10^{-4}	3.5×10^{-4}	4.7×10^{-4}	2.6×10^{-4}
ℓ_u $\left(=\int_0^{\text{first zero}}\langle u(x+r)u(x)\rangle/\langle u^2\rangle\right)$ (m)	0.069	0.12	0.30	0.39
ℓ_v $\left(=\int_0^{\text{first zero}}\langle v(x+r)v(x)\rangle/\langle v^2\rangle\right)$ (m)	0.029	0.064	0.11	0.12
ℓ_θ $\left(=\int_0^{\text{first zero}}\langle \theta(x+r)\theta(x)\rangle/\langle \theta^2\rangle\right)$ (m)	0.057	0.16	0.34	0.44
ℓ' $(=0.9\langle u^2\rangle^{3/2}/\epsilon)$ (m)	0.056	0.14	0.30	0.43
ℓ'_θ $(=\langle\theta^2\rangle^{1/2}/\beta)$ (m)	0.052	0.12	0.33	0.29

which holds in all flows (independent of their degree of homogeneity, isotropy, etc.), given that the above result is purely algebraic.

Because the choice of variable in the above equation is arbitrary, it also can also be written for any scalar field:

$$\langle(\Delta\theta)^3\rangle + 4\langle(\Delta\theta)(\Sigma\theta)^2\rangle = 4\langle(\Delta\theta)\Sigma(\theta^2)\rangle. \tag{8}$$

This being said, a mixed-velocity-passive scalar form of this equation, which pertains to the scale-by-scale transfer of the scalar variance, is more relevant to the present work. It can be derived in a manner analogous to that of Eq. (7), by adding the (algebraic) expansions of $\langle(\Delta u)(\Delta\theta)^2\rangle$ and $\langle(\Delta u)(\Sigma\theta)^2\rangle$. The result is

$$\langle(\Delta u)(\Delta\theta)^2\rangle + 4\langle(\Delta u)(\Sigma\theta)^2\rangle = 4\langle(\Delta u)\Sigma(\theta^2)\rangle, \tag{9}$$

which, we reiterate, has not invoked the assumption of homogeneity. Experimental validation of this relation is shown in Fig. 1, where the two terms on the left-hand side (LHS) are shown as positive and the right-hand side is negative such that the sum of the curves is zero.

Assuming homogeneity in the x direction, Eq. (7) becomes Eq. (5), Eq. (8) becomes

$$\langle(\Delta\theta)(\Sigma\theta)^2\rangle = -\tfrac{1}{12}\langle(\Delta\theta)^3\rangle, \tag{10}$$

and Eq. (9) becomes

$$\langle(\Delta u)(\Sigma\theta)^2\rangle = -\tfrac{1}{4}\langle(\Delta u)(\Delta\theta)^2\rangle + \tfrac{1}{2}\langle u_{x+r}\theta_x^2\rangle - \tfrac{1}{2}\langle u_x\theta_{x+r}^2\rangle, \tag{11}$$

where $u_x = u(x)$, $u_{x+r} = u(x+r)$, and similarly for θ.

Given the $\langle(\Delta u)(\Delta\theta)^2\rangle$ term in the above equation, one can invoke Yaglom's equation [in analogy with the invocation of Kolmogorov's four-fifths law in Eq. (6)], so that, in the inertial-convective

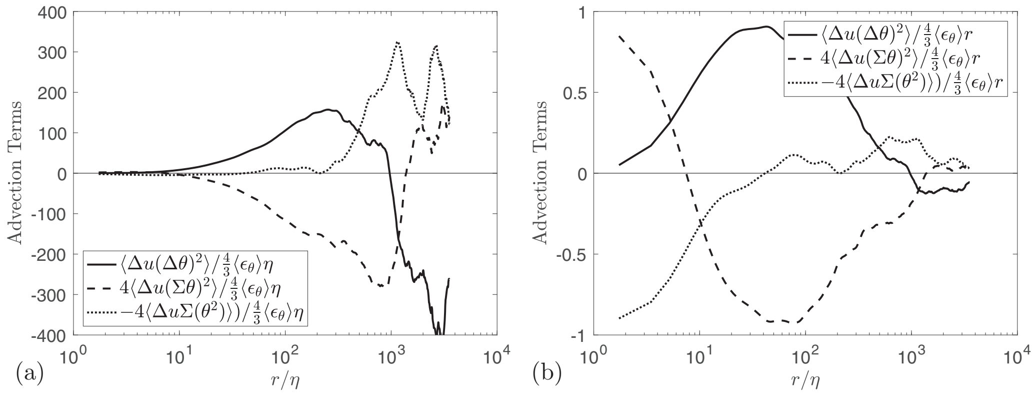

FIG. 1. Scale-by-scale evolution of the terms in Eq. (9) at $R_\lambda = 222$. (a) The terms are nondimensionalized by $\frac{4}{3}\langle\epsilon_\theta\rangle\eta$, which is a constant. (b) The terms are nondimensionalized by $\frac{4}{3}\langle\epsilon_\theta r\rangle$, which is a nondimensionalization that is both a function of scale and analogous with Yaglom's equation.

subrange, Eq. (11) can be rewritten as

$$\langle(\Delta u)(\Sigma\theta)^2\rangle = \tfrac{1}{3}\langle\epsilon_\theta\rangle r + \tfrac{1}{2}\big\langle u_{x+r}\theta_x^2\big\rangle - \tfrac{1}{2}\big\langle u_x\theta_{x+r}^2\big\rangle. \tag{12}$$

We note that Eqs. (8) and (10) are not explicitly equations governing the (advective) transport of the scalar field, given that they do not represent the advection of $\Sigma\theta$ (or $\Delta\theta$ for that matter). The advection of $\Sigma\theta$ (and its relation to that of $\Delta\theta$) is governed by Eq. (9). Furthermore, note the additional terms in Eq. (12), when compared to the analogous expression for the velocity field [Eq. (6)]. These are not present in the analogous equation for the velocity field, as they cancel out when studying "velocity advecting velocity." However, given the necessity of examining mixed velocity-scalar statistics when studying the transport of scalars [27,29], the presence of these additional two terms becomes inevitable. Our last comment with respect to the above equations is that they serve as a guide to the types of statistics that are examined in Secs. III B and III C.

To investigate Eq. (9), we plot the three mixed velocity-temperature structure functions (two mixed IASF/IDSFs and one IDSF) in that equation in Fig. 1. One observes that $4\langle\Delta u\Sigma(\theta^2)\rangle$ balances $\langle(\Delta u)(\Sigma\theta)^2\rangle$ at small scales (i.e., $r/\eta \lesssim 8$), whereas the balance is between $\langle(\Delta u)(\Delta\theta)^2\rangle$ and $4\langle(\Delta u)(\Sigma\theta)^2\rangle$ for larger scales. And while IDSFs are influenced by the fluctuations at scales less than or equal to r, and IASFs are influenced by scales larger than or equal to r, mixed IASF/IDSFs, like $\langle(\Delta u)(\Sigma\theta)^2\rangle$, uniquely depend on the length scale r. But given that the magnitude of fluctuations increases with the scale r, IDSFs like $\langle(\Delta u)(\Delta\theta)^2\rangle$ obtain the majority of their contributions from scales close to r, and can affect the balance between an IDSF and a mixed IASF/IDSF.

B. Incremental average structure functions (IASFs)

As an initial comparison of incremental averages of a passive scalar with those of the velocity field, we plot in Fig. 2(a) the second-order incremental average structure function of the of u, v, and θ for $R_\lambda = 582$, normalized by the variances of the respective quantities. One first observes that the present incremental averages of both u and v are similar to those observed by Mouri and Hori [21]; they decay from a value of 1 in the limit of $r \to 0$ to a value of 1/2 in the limit of $r \to \infty$, as expected. Furthermore, one also notes that (for separations smaller than the integral scale) $\langle(\Sigma_r v)^2\rangle < \langle(\Sigma_r u)^2\rangle$, a result that derives from the larger value of the longitudinal integral scale (ℓ_u) as compared to the transverse one (ℓ_v) in homogeneous, isotropic turbulence [30]. Given that $\ell_v < \ell_u$, $\langle(\Sigma_r v)^2\rangle$ must decay from its small-scale limit (1) to its large-scale limit (1/2) over a shorter range of scales than $\langle(\Sigma_r u)^2\rangle$. The tendency of $\langle(\Sigma_r v)^2\rangle$ to values less than 1/2 at large scales (also observed for the boundary layer and jet data of Mouri and Hori [21], but, interestingly,

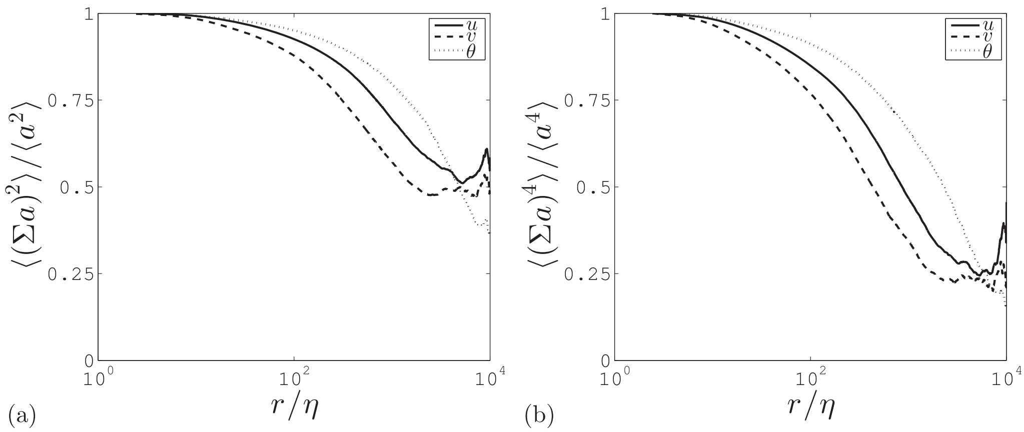

FIG. 2. Normalized (a) second- and (b) fourth-order incremental averages of u, v, and θ. $R_\lambda = 582$.

not their grid turbulence data) can be attributed to the tendency of the autocorrelation of v ($\rho_{vv}(r)$) to become negative at large scales to satisfy continuity (see pp. 252–253 of [30]). With respect to $\langle(\Sigma_r\theta)^2\rangle$, we observe that it is the slowest of the three functions to decay to its asymptotic value, which is consistent with the integral length scale of θ (ℓ_θ) being larger than ℓ_u and ℓ_v. (See Table II.) Fitting a curve of the form given in Table I to the second-order incremental averages results in best-fit scaling exponents, which are given in Table III. Note that these values must be the same as those for the second-order structure function, as is clear from the relations given in Table I.

It is also of interest to consider higher-order incremental averages. To this end, the fourth-order incremental average of u, v, and θ is plotted in Fig. 2(b) for $R_\lambda = 582$. (Note that we do not plot third-order incremental averages, as these are effectively zero, due to the underlying symmetries of the velocity and temperature fields herein.) One observes that the fourth-order incremental averages are quite similar to those at second order. They exhibit the same relative rates of decay towards their asymptotic values, dictated by the relative sizes of the integral length scales for each of the three fields. However, they instead asymptote to a value of approximately 0.25. Note that this latter value is consistent with the large-scale asymptote of $\langle(\Sigma\theta)^4\rangle$, which, if one assumes homogeneity in the x direction and the quasinormal approximation to hold [32,33], gives

$$\begin{aligned}\lim_{r\to\infty}\langle(\Sigma\theta)^4\rangle &= \lim_{r\to\infty}\frac{1}{16}\langle(\theta(x+r)+\theta(x))^4\rangle\\ &= \frac{1}{16}[\langle(\theta(x+r))^4\rangle + 6\langle(\theta(x+r))^2\rangle\langle(\theta(x))^2\rangle + \langle(\theta(x))^4\rangle]\\ &= \frac{1}{16}[\langle(\theta(x+r))^4\rangle + 6(\langle(\theta(x+r))^4\rangle/3)^{1/2}(\langle(\theta(x))^4\rangle/3)^{1/2} + \langle(\theta(x))^4\rangle]\\ &= \frac{4}{16}\langle\theta^4\rangle = \frac{\langle\theta^4\rangle}{4}. \end{aligned} \tag{13}$$

The Reynolds number dependence of the second- and fourth-order incremental average structure functions of temperature are plotted in Figs. 3(a) and 3(b), respectively. The increase in the values of r/η at which the structure function of the incremental average tends to their large-scale asymptotic values increases with Reynolds number, consistent with the increased separation of scales associated with larger Reynolds or Péclet numbers.

In Fig. 4, we proceed to consider the fourth-order incremental average of u, v, and θ nondimensionalized by their respective second-order incremental averages (e.g., $\langle(\Sigma\theta)^4\rangle/\langle(\Sigma\theta)^2\rangle^2$), which we denote as "kurtosis structure functions of incremental averages." As noted by Mouri and Hori [21], these must tend to the kurtosis of the respective quantities (e.g., $\langle\theta^4\rangle/\langle\theta^2\rangle^2$) as $r\to 0$, and

TABLE III. Scaling exponents of the curve fit of the form given in Table I for the second-order incremental average structure functions. Note that this equation renders these values the same as what would be obtained by measuring the scaling exponents of the second-order incremental difference structure functions. The ranges of r/η over which we fit these exponents varied with Reynolds number and quantity (i.e., u, v, or θ) and were calculated using the approach of [31].

R_λ	94	306	582
γ_u	0.50	0.59	0.61
γ_v	0.43	0.55	0.57
γ_θ	0.55	0.60	0.58

to one-half of the kurtosis of the respective quantities plus $\frac{3}{2}$ (e.g., $\langle\theta^4\rangle/(2\langle\theta^2\rangle^2)+\frac{3}{2}$) as $r\to\infty$. Mouri and Hori [21] observed kurtosis structure functions of incremental averages that were constant to within $\pm1\%$, but nevertheless exhibited very similar (small, but consistent) trends for Σu and Σv in grid turbulence, as well as for Σv in their turbulent boundary layer and jet. These were characterized by maxima at $r\sim\ell_u$ and minima at $r\sim10^{-1}\ell_u$. They, however, noted that their observed kurtosis structure functions of Σu were considerably different due to the fact that the kurtosis of the u velocity fluctuation was different from the Gaussian value of 3 (2.69 and 2.60 in the boundary layer and jet, respectively). In the present experiments, the variation of the kurtosis structure functions of incremental averages is substantially larger than the $\pm1\%$ variation with r/η observed by Mouri and Hori [21]. Although one might be tempted to associate this increased variation with the intense, unsteady fluctuations associated with active-grid generated turbulence, this larger variation of kurtosis structure functions of incremental averages is also observed for the lower-Reynolds-number data set studied herein, generated by means of a passive grid. In the present work, the kurtosis structure functions of incremental averages of the v component of velocity [Fig. 4(b)] exhibit the smallest variations with r/η. Nevertheless, like in the work of Mouri and Hori [21], they too are affected, at all scales, by the value of the kurtosis of v. Perhaps more interestingly, we observe that the kurtosis structure function that exhibits the largest variation with r/η is that corresponding to temperature [Fig. 4(c)]. We hypothesize that this larger variation of $\langle(\Sigma\theta)^4\rangle/\langle(\Sigma\theta)^2\rangle^2)$ with r/η is associated

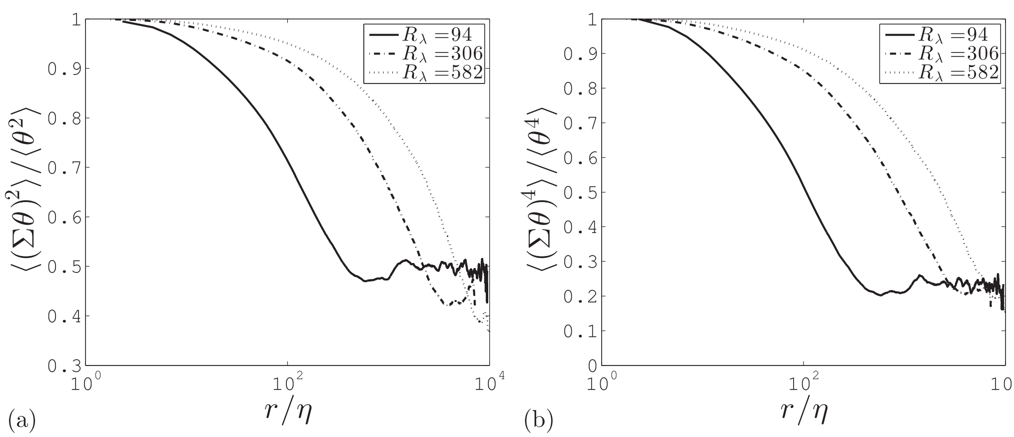

FIG. 3. Reynolds number dependence of the normalized (a) second- and (b) fourth-order incremental average structure functions of temperature.

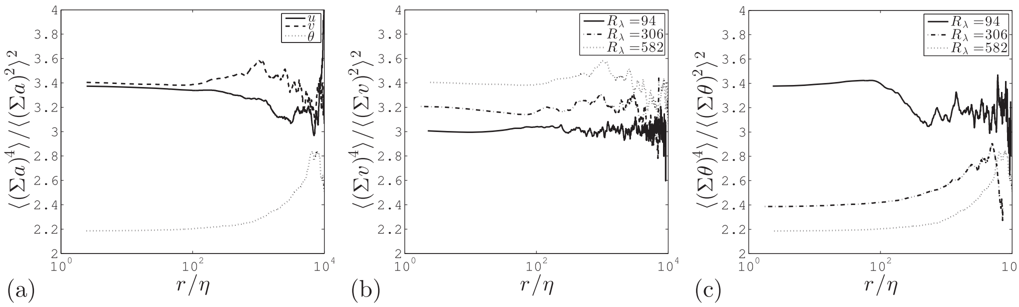

FIG. 4. Kurtosis structure functions of incremental averages. (a) $\langle(\Sigma u)^4\rangle/\langle(\Sigma u)^2\rangle^2$, $\langle(\Sigma v)^4\rangle/\langle(\Sigma v)^2\rangle^2$, and $\langle(\Sigma\theta)^4\rangle/\langle(\Sigma\theta)^2\rangle^2$ for $R_\lambda = 582$. (b) The Reynolds number dependence of $\langle(\Sigma v)^4\rangle/\langle(\Sigma v)^2\rangle^2$. (c) The Reynolds number dependence of $\langle(\Sigma\theta)^4\rangle/\langle(\Sigma\theta)^2\rangle^2$.

with the intimate connection between the evolution of passive scalar fields and the passive scalar initial conditions [34,35].

Given that turbulent transport of temperature fluctuations (i.e., the turbulent convective heat transfer) is (i) effected by the action of the turbulent velocity fluctuations against the mean temperature gradient, and (ii) a large-scale phenomenon, it is of interest to examine the mixed (second-order) velocity-temperature IASFs: $\langle\Sigma v \Sigma\theta(r)\rangle/\langle v\theta\rangle$. We only consider the quantity dependent upon the v component of velocity, as that is the only one affecting net heat transfer given that the mean temperature gradient is solely in the y direction. $\langle\Sigma v \Sigma\theta(r)\rangle/\langle v\theta\rangle$ is plotted in Fig. 5 for three different Reynolds numbers. One observes that these mixed velocity-temperature IASFs are similar to the respective second-order IASFs of their constituent components (i.e., v and θ). In general, it seems that IASFs of passive scalar fields behave similarly to those of the velocity field, even if the nature of the field is quite different (i.e., isotropic vs anisotropic, with production vs.without production, etc.). This may be attributable to the small- and large-scale limits of IASFs, which are the same for all fields, and which therefore enforce a consistency in their form. However, the latter is invariably Reynolds- and Péclet-number dependent, akin to what is also observed for IDSFs [31,36,37].

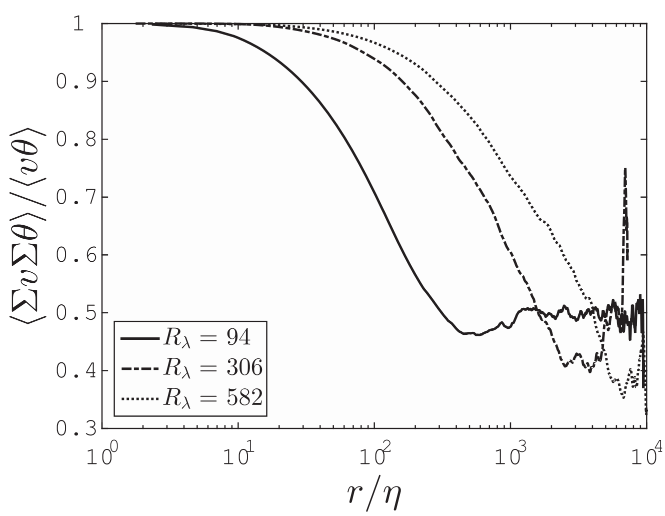

FIG. 5. Normalized, mixed velocity-temperature second-order incremental average structure function $(\Sigma v \Sigma\theta)$.

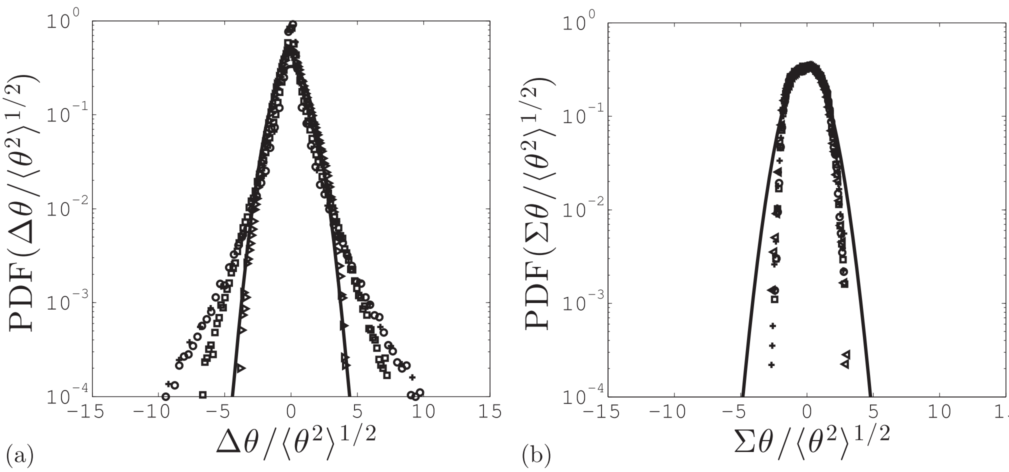

FIG. 6. Probability density function for the first-order structure function of (a) the incremental difference and (b) the incremental average at $R_\lambda = 582$. Circles, $r = 10\eta$; squares, $r = 100\eta$; triangles, $r = 1000\eta$; crosses, (a) PDF($\frac{\partial\theta}{\partial x}/\langle(\frac{\partial\theta}{\partial x})^2\rangle$) and (b) PDF($\theta/\theta_{\rm rms}$). The solid lines are Gaussian fits to the (a) incremental difference at $r/\eta = 1000$ (mean, 0; standard deviation, 1.1) and (b) incremental average at $r/\eta = 1000$ (mean, -0.01; standard deviation, -1.2).

C. Probability density functions and conditional expectations of incremental averages

Given the contrast between the previously observed structure functions of incremental averages and those of differences, it is of interest to study the PDFs of incremental averages, which are plotted in Fig. 6. As is well known [9,38], the PDF of incremental differences (e.g., $\Delta\theta$) changes with the scale under consideration, evolving from being quasi-Gaussian in shape at large separations to being super-Gaussian for small increments, due to the effects of internal intermittency. On the other hand, one observes that the PDF of $\Sigma\theta$ does not vary with r/η, as incremental differences are dominated by their large-scale behavior [21]. As can be seen in Fig. 6(b), the PDF of $\Sigma\theta$ is nearly identical to the PDF of $\theta/\theta_{\rm rms}$, consistent with the results of Sreenivasan and Dhruva [12] for the velocity field. Note that the PDF of $\theta/\theta_{\rm rms}$ in this active-grid-generated flow is somewhat sub-Gaussian, due to the large integral length scale relative to the wind tunnel width (see [6]).

We extend this analysis to joint probability density functions (JPDFs) of incremental averages of different quantities. To be able to sensibly interpret JPDFs of incremental averages, we first plot the (normalized) JPDFs of u and v, u and θ, as well as v and θ in Figs. 7(a)–7(c), respectively, for $R_\lambda = 582$. We then proceed to plot (normalized) JPDFs of Σu and Σv, Σu and $\Sigma\theta$, and Σv and $\Sigma\theta$ in Figs. 7(d)–7(f), respectively (for $r/\eta = 100$ and $R_\lambda = 582$). We remark that for a normalized joint-Gaussian distribution, circular contour lines indicate a lack of correlation between the two variables, and that statistical correlation is evidenced by contour lines that are elliptical with major axes parallel to (i) $y = x$, for variables that are positively correlated, and (ii) $y = -x$, for variables that are negatively correlated. This is most clearly demonstrated by the negative correlation between v and θ in Fig. 7(c).

From Fig. 7, one observes that the JPDFs of the incremental averages are quite similar to their large-scale analogs (i.e., the JPDFs of u, v, and θ). Furthermore, the relative insensitivity of JPDFs to the separation was confirmed by measurements performed at different separations and Reynolds numbers (not shown) and is consistent with the PDFs of Σu, Σv, and $\Sigma\theta$, which were notably (i) scale independent and (ii) different from the PDFs of Δu, Δv, and $\Delta\theta$, which are strongly scale dependent.

Conditional expectations of incremental averages are of further interest to examine, especially given their recent use in determining the effect of large-scale quantities on the small-scale structure

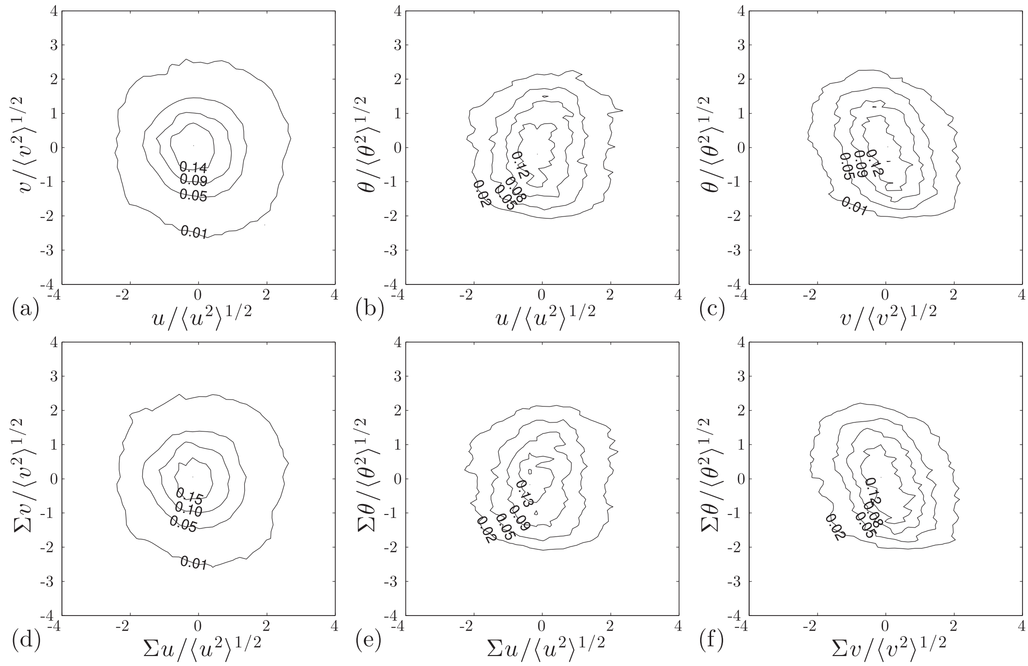

FIG. 7. Joint probability density functions of (a) u and v, (b) u and θ, (c) v and θ, (d) Σu and Σv, (e) Σu and $\Sigma\theta$, and (f) Σv and $\Sigma\theta$. $R_\lambda = 582$. $r/\eta = 100$.

of a flow (e.g., [18,19]). As previously noted, Mouri and Hori [21] calculated the average of the (squared) incremental average of the longitudinal velocity fluctuation conditioned upon its difference over the same separation ($\langle(\Sigma u)^2|\Delta u\rangle$) in grid turbulence, a boundary layer, and a turbulent jet to further investigate the (nonzero) correlation between Σu and Δu, given by Eq. (5). A related statistic, $\langle(\Delta u)^2|\Sigma u\rangle$, was calculated in Ref. [19] to investigate the effects of the large scales on the small-scale statistics in a variety of turbulent flows. Mouri and Hori [21] observed a clear difference in the behavior of $\langle(\Sigma u)^2|\Delta u\rangle$ in grid turbulence as compared to that observed in a boundary layer and a turbulent jet. This difference is discussed shortly in relation to the analogous measurements of incremental averages in hydrodynamic and scalar fields.

In the present work, we examine $\langle(\Sigma u_\alpha)^2|\Delta u_\alpha\rangle$, $\langle(\Sigma\theta)^2|\Delta\theta\rangle$, and $\langle(\Sigma\theta)^2|\Delta u\rangle$ in Figs. 8 and 9. We observe good agreement between the present conditional expectations of Σu and those of Mouri

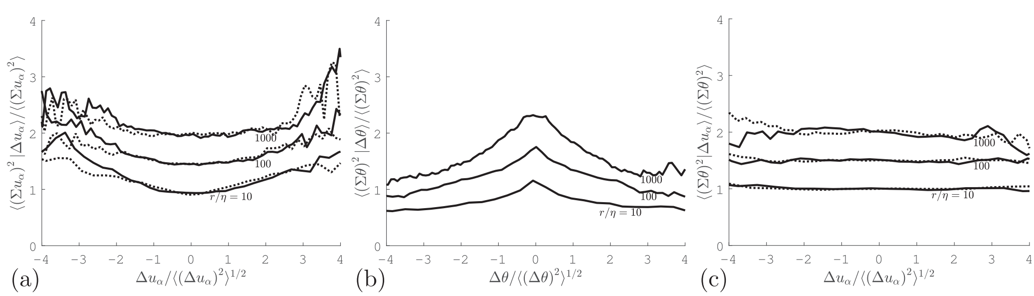

FIG. 8. Scale dependence of the (nondimensionalized) expectations of (a) $\langle(\Sigma u_\alpha)^2|\Delta u_\alpha\rangle$, (b) $\langle(\Sigma\theta)^2|\Delta\theta\rangle$, and (c) $\langle(\Sigma\theta)^2|\Delta u_\alpha\rangle$. In (a) and (c), the solid line represents data for which $u_\alpha = u$ (the longitudinal velocity fluctuation), and the dashed line represents $u_\alpha = v$ (the transverse velocity fluctuation). $r = 10\eta$ (bottom), $r = 100\eta$ (middle, offset by 0.5), and $r = 1000\eta$ (top, offset by 1.0). $R_\lambda = 582$.

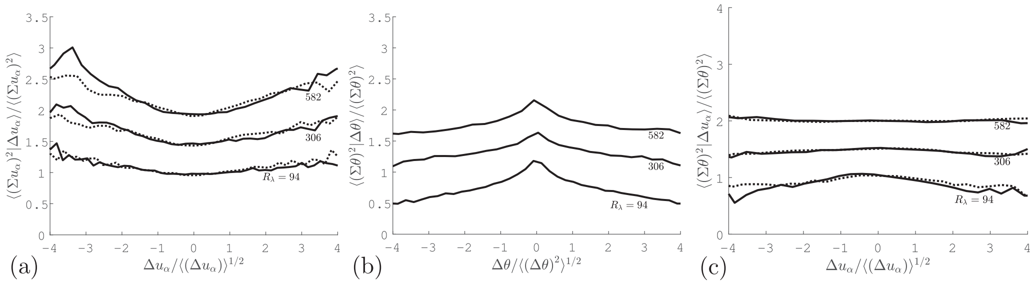

FIG. 9. Reynolds-number dependence of the nondimensionalized expectations of (a) $\langle(\Sigma u_\alpha)^2|\Delta u_\alpha\rangle$, (b) $\langle(\Sigma\theta)^2|\Delta\theta\rangle$, and (c) $\langle(\Sigma\theta)^2|\Delta u_\alpha\rangle$. In (a) and (c), the solid line represents data for which $u_\alpha = u$ (the longitudinal velocity fluctuation), and the dashed line represents $u_\alpha = v$ (the transverse velocity fluctuation). $R_\lambda = 94$ (bottom), $R_\lambda = 306$ (middle, offset by 0.5), and $R_\lambda = 582$ (top, offset by 1.0). $r/\eta = 10$.

and Hori [21] measured in grid turbulence. Furthermore, note that the conditional expectations of Σv follow a similar behavior to those of Σu, albeit more symmetric, given the lack of any (known) relationship of the form of Eq. (5) existing for the *transverse* velocity fluctuation. The asymmetry in these plots is related to the nonzero correlation between the incremental averages and differences (see [21]). However, the expectations of $\Sigma\theta$, conditioned upon $\Delta\theta$, are distinctly different than the analogous ones for the velocity field. Whereas the latter are concave up, plots of $\langle(\Sigma\theta)^2|\Delta\theta\rangle$ are clearly concave down, indicating that large values of $\Delta\theta$ are associated with small values of $\Sigma\theta$, and vice versa. In fact, the present measurements of $\langle(\Sigma\theta)^2|\Delta\theta\rangle$ resemble the measurements of $\langle(\Sigma u_\alpha)^2|\Delta u_\alpha\rangle$ in the jet and boundary layer flows of Mouri and Hori [21], who hypothesized that their observed differences in $\langle(\Sigma u_\alpha)^2|\Delta u_\alpha\rangle$ for measurements in (i) grid turbulence and (ii) jet and boundary layer turbulence were due to the effects of turbulent production, which predominantly affect the largest scales. This explanation is consistent with the present scalar-field measurements, given that the temperature fluctuations in the present flow are produced by the turbulent velocity fluctuations acting on the mean scalar gradient. Consequently, the role of turbulent production (or presumably any other large-scale turbulent mechanism, such as decay or inhomogeneity) is important in the evolution of statistics of incremental averages, whether they be hydrodynamic or scalar. This being said, we remark that the dependence of $\langle(\Sigma\theta)^2|\Delta\theta\rangle$ on the separation (r/η) in the present work [Fig. 8(b)] is weaker than that observed for $\langle(\Sigma u_\alpha)^2|\Delta u_\alpha\rangle$ in the jet and boundary layer of Mouri and Hori [21]. Whereas the jet and boundary layer data of Mouri and Hori [21] exhibit a strong evolution with r/η over the range $10^1 < r/\eta < 10^3$, the present results for $\langle(\Sigma\theta)^2|\Delta\theta\rangle$ show a much weaker dependence on r/η, with the shapes of $\langle(\Sigma\theta)^2|\Delta\theta\rangle$ for all three separations ($r/\eta = 10$, 100, and 1000) most closely resembling the results of Mouri and Hori [21] at $r/\eta = 1000$. This may be tied to the known connection between large and small scales of passive scalar fields (e.g., ramp-cliff structures [5,9,10]).

The Reynolds-number dependence of $\langle(\Sigma u_\alpha)^2|\Delta u_\alpha\rangle$ and $\langle(\Sigma\theta)^2|\Delta\theta\rangle$ is shown in Fig. 9. The dependence of $\langle(\Sigma u_\alpha)^2|\Delta u_\alpha\rangle$ and $\langle(\Sigma\theta)^2|\Delta\theta\rangle$ on R_λ is especially weak—a fact that is somewhat surprising given the (partially) large-scale nature of these statistics, which may not necessarily be flow independent.

D. Extension of Yaglom's equation

Given that $\langle(\Sigma\theta)^2\rangle$ is a second-order statistic that is a function of the scale over which it is measured, it is of interest to consider its scale-by-scale budget. The objective of this section is thus to derive a scalar budget written in terms of the incremental average, analogous to Yaglom's equation [39] (the scale-by-scale budget of the scalar variance, written in terms of the incremental difference).

Using the same procedure as outlined by Danaila and Mydlarski [22] for incremental differences, we write the advection-diffusion equation for the instantaneous scalar field θ_t at two points $\vec{x}$ and

$\vec{x}^+$, which are separated by the increment $\vec{r} = \vec{x}^+ - \vec{x}$ and where the subscript t denotes "total":

$$\partial_t \theta_t + u_{i,t} \partial_i \theta_t = \kappa \partial_i^2 \theta_t \tag{14}$$

and

$$\partial_t \theta_t^+ + u_{i,t}^+ \partial_i^+ \theta_t^+ = \kappa \partial_i^{2+} \theta_t^+. \tag{15}$$

The superscript + refers to quantities evaluated at $\vec{x}^+$. In Eqs. (14) and (15), $u_{i,t}$ is the instantaneous velocity vector, $\partial_t \equiv \partial/\partial t$, $\partial_i \equiv \partial/\partial x_i$, and ∂_i^2 is the Laplacian, $\partial^2/\partial x_i^2$. Hereinafter, the notation ∂_i and ∂_i^+ is used to denote derivatives with respect to x_i and x_i^+, respectively. When other spatial variables are involved, the derivatives are written explicitly, e.g., $\partial/\partial r_i$.

We assume that $u_{i,t}$ and θ_t depend upon $\vec{x}$ and *not* $\vec{x}^+$. Analogously, we also assume that $u_{i,t}^+$ and θ_t^+ depend upon $\vec{x}^+$ and *not* $\vec{x}$. Furthermore, decomposing the total velocity field into mean and fluctuating components leads to $u_{i,t} = U_i + u_i$, $u_{i,t}^+ = U_i^+ + u_i^+$, $\theta_t = T + \theta$, and $\theta_t^+ = T^+ + \theta^+$.

Adding Eqs. (14) to (15) then dividing by 2 yields an equation for the temperature IASF ($\Sigma\theta$), viz.,

$$\begin{aligned} &D/Dt(\Sigma\theta) + \Sigma(U_i \partial_i T) + \Sigma(u_i \partial_i T) + u_i^+ \partial_i^+ (\Sigma\theta) + u_i \partial_i (\Sigma\theta) \\ &\quad = \kappa \big(\partial_i^2 + \partial_i^{2+}\big)(\Sigma\theta) + \kappa \partial_i^{2+} T^+ + \kappa \partial_i^2 T, \end{aligned} \tag{16}$$

where $\Sigma a \equiv (a + a^+)/2$ and $Da/Dt \equiv \partial_t a + U_i \partial_i a$, for an arbitrary field a. Moreover, note that U_i and T are, respectively, the mean velocity and temperature, for which statistical stationarity is assumed in both frames of reference, so that $\partial_t U_i = \partial_t U_i^+ = \partial_t T = \partial_t T^+ \equiv 0$. We also suppose that $\partial_i^2 T = \partial_i^{2+} T^+ \equiv 0$ (because T is a linear function of y, and independent of x and z), and that $\partial_\alpha T = \partial_\alpha^+ T^+$ (the mean temperature gradient is the same at $\vec{x}$ and $\vec{x}^+$).

Following the approach suggested by Hill [40], we consider the gradient with respect to the midpoint of the interval:

$$\vec{X} = \tfrac{1}{2}(\vec{x} + \vec{x}^+), \tag{17}$$

such that

$$\partial_\alpha^+ \equiv \frac{\partial}{\partial r_\alpha} + \frac{1}{2}\partial_{X_\alpha}, \tag{18}$$

$$\partial_\alpha \equiv -\frac{\partial}{\partial r_\alpha} + \frac{1}{2}\partial_{X_\alpha}, \tag{19}$$

resulting in $\partial_{X_\alpha} = \partial_\alpha + \partial_\alpha^+$.

By taking into account Eq. (18), multiplying Eq. (16) by $2\Sigma\theta$, and averaging, we finally obtain

$$\begin{aligned} &D_t \langle (\Sigma\theta)^2 \rangle(\vec{r}) + 2\langle \Sigma u_i \Sigma\theta \rangle \partial_i T(\vec{r}) + \frac{1}{2}\langle [\partial_i + \partial_i^+][u_i + u_i^+](\Sigma\theta)^2 \rangle(\vec{r}) + \frac{\partial}{\partial r_i}\langle \Delta u_i (\Sigma\theta)^2 \rangle(\vec{r}) \\ &= 2\kappa \frac{\partial^2}{\partial {r_i}^2}\langle (\Sigma\theta)^2 \rangle(\vec{r}) - \frac{1}{2}(\langle \epsilon_\theta \rangle + \langle \epsilon_\theta \rangle^+). \end{aligned} \tag{20}$$

Note that the first line in Eq. (20) corresponds to large-scale effects. More specifically, the first term represents the nonstationarity and/or advection by way of the mean velocity, the second one is a production term, and the third one pertains to the turbulent diffusion. In Eq. (20), each term depends on the spatial vector $\vec{r}$. Special attention should be paid to the last term, e.g., $\langle \epsilon_\theta \rangle + \langle \epsilon_\theta \rangle^+$, which also depends on the vector $\vec{r}$. We now proceed to write Eq. (20) as

$$D + P + Td + \frac{\partial}{\partial r_i}\langle \Delta u_i (\Sigma\theta)^2 \rangle(\vec{r}) = 2\kappa \frac{\partial^2}{\partial {r_i}^2}\langle (\Sigma\theta)^2 \rangle(\vec{r}) - \frac{1}{2}(\langle \epsilon_\theta \rangle + \langle \epsilon_\theta \rangle^+), \tag{21}$$

where the first term on the LHS of Eq. (21) is the decay term (D), the second one is the production term (P), and the third one is the turbulent diffusion term, Td. All the others are the classical terms, analogous to those in Yaglom's equation, that are therefore treated in the classical manner [22]. Also note that both the small- and large-scale limits of Eq. (21) are consistent with the one-point energy budget equation. Moreover, recall that in the large-scale limit ($r \to \infty$) the scale-by-scale budget equation simplifies to the one-point energy (scalar variance) budget, whereas in the small-scale limit it reduces to the evolution equation of the mean dissipation rate of the scalar variance, $\langle \epsilon_\theta \rangle$. Therefore, the requirement that Eq. (21) be balanced at small scales imposes a stronger constraint—a discussion to which we return in the context of the experimentally obtained results.

We further note, in the context of the locally stationary, homogenous (region of the) flow, that the flow is statistically stationary at a given position, so that time derivatives of any time-averaged statistics are zero. The first term is therefore equal to $U_i \partial_i \langle (\Sigma\theta)^2 \rangle (\vec{r})$.

Terms in Eq. (21) can be evaluated from either direct numerical simulations, or combined planar velocity and scalar measurements (e.g., planar laser-induced fluorescence combined with particle image velocimetry). In the present work, we evaluate terms in Eq. (21) from (one-point) simultaneous hot- and cold-wire measurements. This approach does not allow us to estimate the real, spatial variation of these terms (without performing concurrent measurements at two points in space, thus involving two X wires and two cold wires operating simultaneously). Given this context, our approach involves assuming all extra terms take on an isotropic form. Their estimation from experimental (hot- and cold-wire) data implicitly assumes that the two reference systems are actually identical, and the spatial increments and/or IASFs at a scale r are estimated using Taylor's hypothesis, which imposes homogeneity at all scales.

For relatively small scales, the molecular diffusion and the advection terms are considered as being locally isotropic and therefore only depend on r (the modulus of the separation $\vec{r}$). Thus, the divergence and Laplacian operators assume particular forms under these conditions. Note that the hypothesis of local isotropy of $\langle (\Sigma\theta)^2 \rangle$ is less likely to be accurate than the same hypothesis for $\langle (\Delta\theta)^2 \rangle$ because the former includes all scales larger than a given scale r (which are more likely anisotropic), whereas the latter pertains to the scales smaller than or equal to r.

For increasingly large scales, different terms in Eq. (21) tend to constants, and their spatial dependence is no longer observed, as discussed in Ref. [22]. Therefore, application of local isotropy in our present approach does not ignore the anisotropy of the flow, and our approach is not overly sensitive to this assumption.

Therefore, under the assumption of local isotropy, the terms D, P, and Td can be considered independent of the spatial orientation. Our last hypothesis is that the variations in $\langle \epsilon_\theta \rangle$ over scales smaller than L (the integral scale) are negligible so that $\langle \epsilon_\theta \rangle = \langle \epsilon_\theta \rangle^+$. Thus, the term containing the two-point mean dissipation rate, $\langle \epsilon \rangle + \langle \epsilon \rangle^+$, does not depend on the spatial orientation ($\vec{r}$).

Since all the terms in Eq. (21) now only depend on r, suitable expressions for the divergence and Laplacian operators can be chosen (namely, those corresponding to a spherical coordinate system). By following the classical approach [22], we finally obtain

$$-\langle \Delta u_1 (\Sigma\theta)^2 \rangle + 2\kappa \frac{d}{dr} \langle (\Sigma\theta)^2 \rangle - \frac{U_1}{r^2} \int_0^r s^2 \partial_1 \langle (\Sigma\theta)^2 \rangle ds$$
$$-\frac{2}{r^2} \int_0^r s^2 \left[\frac{\partial T}{\partial x_2} \langle \Sigma u_2 \Sigma\theta \rangle + \partial_2 \langle (\Sigma u_2)(\Sigma\theta)^2 \rangle \right] ds = \frac{1}{3} \langle \epsilon_\theta \rangle r, \tag{22}$$

where s is a dummy variable. As shown by Danaila and Mydlarski [22], turbulent diffusion is negligible in the flow under investigation at the level of the one-point energy budget equation, which represents the large-scale limit of Eq. (22). The final transport equation for $\langle (\Sigma\theta)^2 \rangle$ is

$$-\langle \Delta u_1 (\Sigma\theta)^2 \rangle + 2\kappa \frac{d}{dr} \langle (\Sigma\theta)^2 \rangle - \frac{U_1}{r^2} \int_0^r s^2 \partial_1 \langle (\Sigma\theta)^2 \rangle ds - \frac{2}{r^2} \frac{\partial T}{\partial x_2} \int_0^r s^2 [\langle \Sigma u_2 \Sigma\theta \rangle] ds = \frac{1}{3} \langle \epsilon_\theta \rangle r. \tag{23}$$

At this point, a reasonable assumption can be made about the character of the second-order moment of the scalar incremental difference. Following the approach of Danaila *et al.* [41], we

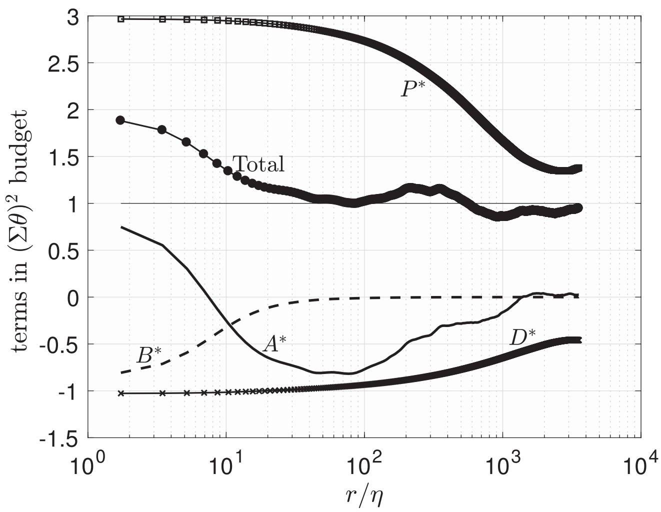

FIG. 10. Scale-by-scale evolution of the terms in Eq. (26). $R_\lambda = 222$.

assume a self-similar behavior of the downstream evolution of structure functions such that they can be written as

$$\langle(\Sigma\theta)^2\rangle(r, x_1) = f(r)g(x_1). \tag{24}$$

Suitable choices for $f(r)$ and $g(x_1)$ are

$$f(r) = \frac{\langle(\Sigma\theta)^2\rangle}{\langle\theta^2\rangle} = \text{const},$$

$$g(x_1) = \langle\theta^2\rangle.$$

Implementing this assumption, the final form of the transport equation for $\langle(\Sigma\theta)^2\rangle$ becomes

$$-\langle\Delta u_1(\Sigma\theta)^2\rangle + 2\kappa\frac{d}{dr}\langle(\Sigma\theta)^2\rangle - \frac{U_1}{r^2}\partial_1\langle\theta^2\rangle\int_0^r s^2\frac{\langle(\Sigma\theta)^2\rangle}{\langle\theta^2\rangle}ds - \frac{2}{r^2}\frac{\partial T}{\partial x_2}\langle u_2\theta\rangle\int_0^r s^2\left[\frac{\langle\Sigma u_2\Sigma\theta\rangle}{\langle u_2\theta\rangle}\right]ds$$
$$= \frac{1}{3}\langle\epsilon_\theta\rangle r. \tag{25}$$

After dividing by $\langle\epsilon_\theta\rangle r$ and multiplying by 3, this equation can be written in the following dimensionless form:

$$A^* + B^* + D^* + P^* = 1, \tag{26}$$

where A^* is the (nondimensional) advection term, B^* is the molecular one, D^* is the inhomogeneous ("decay") term in the streamwise direction x_1, and P^* is the production term.

This scalar budget, corresponding to Eq. (26), is plotted in Fig. 10. (Note that both downstream and transverse measurements were made, such that quantities like $\partial\langle\theta^2\rangle/\partial x_1$ and $\partial T/\partial x_2$ were evaluated from experimental data.) Taking into consideration that $\langle(\Sigma\theta)^2\rangle$ represents the total scalar variance at all scales larger than or equal to r, the physical significance can be considered. Specifically, the total scalar variance transferred towards smaller scales by all scales $\geqslant r$, i.e., terms proportional to $\langle\epsilon_\theta\rangle$, is composed of four types of contributions:

(i) positive contribution due to the variance produced in the flow at scales larger than or equal to r (term P^*).

(ii) negative contribution due to the molecular diffusion (term B^*).

(iii) negative contribution due to the decay effect (term D^*). Recall that the scalar variance increases in the downstream direction in this flow, unlike for the velocity field grid turbulence. This is due to the presence of the mean scalar gradient, which continuously injects scalar fluctuations in the flow.

(iv) negative contribution over the majority range of scales (term A^*), which correspond to the energy transferred through turbulence. However, for the smallest scales (here, smaller than 8η), this term changes its sign and its value is $-\langle \Delta u (\Delta\theta)^2 \rangle$. The physical signification of term A^* is directly related to the balance between $-\langle \Delta u (\Delta\theta)^2 \rangle$ and $\langle \Delta u \Sigma(\theta^2) \rangle$, as reflected by Eq. (9) and Fig. 1.

Finally, we both note and explain the origin of the disagreement between Eq. (26) and the experimental data at small scales. Scale-by-scale equations for incremental differences, by definition, reduce to the definition of the dissipation rate of turbulent kinetic energy, or scalar variance, which is well validated experimentally [22]. In the present case, as already stated and in contrast with the scale-by-scale equations for incremental differences, the small-scale limit of Eq. (26) reduces to the sum of (i) the definition of the dissipation rate of turbulent kinetic energy, or scalar variance, and (ii) the one-point turbulent scalar variance budget, which has contributions from all scales.

One might therefore hypothesize that this disagreement between Eq. (26) and the experimental data at small scales is due to a combined effect of (i) residual anisotropy and (ii) a loss of accuracy in an assumption made when deriving Eq. (26).

Specifically, the two measurements in our incremental average are no longer statistically independent at small separations (i.e., as $\vec{r}$ tends to zero), which conflicts with the assumption that the two points $\vec{x}$ and $\vec{x}^+$ are independent (i.e., $u_{i,t}$ and θ_t depend only on $\vec{x}$, and $u_{i,t}^+$ and θ_t^+ depend only on $\vec{x}^+$)—an assumption used in both the derivation of Eq. (26), as well as that of the scale-by-scale equations for incremental differences. When $\vec{r} = 0$, this assumption fails completely because the two points are coincident (identical). This unique phenomenon does not arise when considering incremental differences, because the averages cancel out and the scale-by-scale evolution equation of incremental differences reduces to the evolution equation of $\langle \epsilon \rangle$ or $\langle \epsilon_\theta \rangle$. When considering incremental sums rather than differences, the averages do not cancel and are therefore correlated at small scales, in contradiction with the assumption underlying the derivation of Eq. (26).

If one does not make the hypothesis that the two quantities are independent in deriving Eq. (26), one obtains

$$A^* + M^* + D^* + P^* = 1, \tag{27}$$

where the molecular term $M^* = 3M/(\langle \epsilon_\theta \rangle r)$ [which replaces the term B^* in Eq. (26)] and M is given by

$$M = \frac{1}{r^2}\int_0^r s^2\left[\left\langle \frac{\partial\theta}{\partial x_j}\frac{\partial\theta^+}{\partial x_j}\right\rangle + \left\langle \frac{\partial\theta^+}{\partial x_j^+}\frac{\partial\theta}{\partial x_j^+}\right\rangle\right]ds = \frac{2}{r^2}\int_0^r s^2\left[\left\langle \frac{\partial\theta}{\partial x_j}\frac{\partial\theta^+}{\partial x_j}\right\rangle\right]ds. \tag{28}$$

When the two points are statistically independent, the term $\langle \frac{\partial\theta}{\partial x_j}\frac{\partial\theta^+}{\partial x_j} \rangle$ is equal to zero. However, when $r \to 0$, this term becomes proportional to the dissipation rate of the scalar variance and balances the budget equation. The lack of statistical independence at small scales could also contaminate the advection term (A^*) and require a similar analysis, although we do not do so herein, because the advection term is present at all scales, and for most of them the two frames are indeed independent. The correlation between two points at small separations offers a new perspective on the statistical approach to understanding turbulent quantities at a scale r such as $\Sigma\theta$ or any other quantity that is more complex than classical incremental differences.

IV. CONCLUSIONS

In conclusion, we have investigated the statistics of incremental averages of a turbulent passive scalar for the first time. We studied both their spatial (i.e., r/η) and Reynolds-number dependence, as well as certain relevant mixed (velocity-temperature) statistics of incremental averages. In doing so, we derived a passive scalar analog to Hosokawa's equation.

Although statistics of incremental averages are *primarily* large-scale quantities, and thus expected to be flow dependent, the statistics of incremental averages of passive scalars measured herein exhibit many similarities to those of the velocity field in different flows. Nevertheless, the similarities are not universal and certain statistics exhibit distinct differences from the velocity field. Furthermore, although IASFs are dictated by the scales larger than or equal to r, it is predominantly the largest scales that contribute to their behavior, as was clearly demonstrated by the PDFs and JPDFs. Conditional expectations of $\Sigma\theta$, conditioned upon $\Delta\theta$, were found to be distinctly different than the analogous ones for the velocity field, and more closely resembled the conditional expectations $\langle(\Sigma u_\alpha)^2|\Delta u_\alpha\rangle$ measured in the jet and boundary layers (i.e., shear) flows of Mouri and Hori [21], and may be tied to the presence of mean (i.e., large-scale) gradients of temperature and velocity, respectively.

We also derived a scale-by-scale evolution equation for the incremental average of passive scalars, similar to Yaglom's equation. Agreement of the data was reasonable, given the assumptions involved in the derivation, and those used in the analysis of our (one-point) data.

Future studies of incremental averages may want to further study and quantify the effect of the assumption of statistical independence of quantities measured at $\vec{x}$ and $\vec{x}^+$ as $\vec{r} \to 0$. Moreover, it may also be of interest to examine the effect of the nature of the large scales of the (scalar) field (i.e., its generation mechanism) on the structure and evolution of IASFs. For example, scale-by-scale budgets of $\langle(\Sigma\theta)^2\rangle$ could be derived for flows in which the large scales are inhomogeneous, as opposed to the homogeneous flow studied herein. Such an extension of this work may be fruitful, given the (i) similarities observed in the statistics of $\langle(\Sigma\theta)^2\rangle$ presented herein, as well as those of $\langle(\Sigma u_\alpha)^2\rangle$ presented by Mouri and Hori [21] in jet and boundary layer flows—flows in which fluctuations are produced by mean gradients—and (ii) differences with the velocity IASFs measured in homogeneous, isotropic grid turbulence, both herein and by Mouri and Hori [21]. Such studies could, hopefully, indicate whether any possibility exists that IASFs may exhibit a potential universal behavior, or whether they are invariably Reynolds- or Péclet-number dependent, given their contribution from scales greater than or equal to r.

ACKNOWLEDGMENTS

This work was funded by the Natural Sciences and Engineering Research Council of Canada (Grant No. RGPIN 217184), as well as by the CORIA and the LabEx EMC3, while L.M. was graciously hosted there while on sabbatical leave. C.R.M. was supported by a US NSF Graduate Research Fellowship under Grant No. DGE1144152.

[1] A. Kolmogorov, The local structure of turbulence in incompressible viscous fluid for very large Reynolds numbers, Dokl. Akad. Nauk. SSSR **30**, 301 (1941).

[2] A. M. Oboukhov, Structure of the temperature field in turbulent flows, Izv. Akad. Nauk. SSSR, Geogr. Geofiz. **13**, 58 (1949).

[3] S. Corrsin, On the spectrum of isotropic temperature fluctuations in an isotropic turbulence, J. Appl. Phys. **22**, 469 (1951).

[4] Jayesh, C. Tong, and Z. Warhaft, On temperature spectra in grid turbulence, Phys. Fluids **6**, 306 (1994).

[5] C. Tong and Z. Warhaft, On passive scalar derivative statistics in grid turbulence, Phys. Fluids **6**, 2165 (1994).

[6] L. Mydlarski and Z. Warhaft, Passive scalar statistics in high-Péclet-number grid turbulence, J. Fluid Mech. **358**, 135 (1998).

[7] L. Mydlarski and Z. Warhaft, Three-point statistics and the anisotropy of a turbulent passive scalar, Phys. Fluids **10**, 2885 (1998).

[8] K. R. Sreenivasan, On local isotropy of passive scalars in turbulent shear flows, Proc. R. Soc. London A **434**, 165 (1991).
[9] Z. Warhaft, Passive scalars in turbulent flows, Annu. Rev. Fluid Mech. **32**, 203 (2000).
[10] B. I. Shraiman and E. D. Siggia, Scalar turbulence, Nature (London) **405**, 639 (2000).
[11] P. E. Dimotakis, Turbulent mixing, Annu. Rev. Fluid Mech. **37**, 329 (2005).
[12] K. Sreenivasan and B. Dhruva, Is there scaling in high-Reynolds-number turbulence? Prog. Theor. Phys. **130**, 103 (1998).
[13] T. Tatsumi and T. Yoshimura, Inertial similarity of velocity distributions in homogeneous isotropic turbulence, Fluid Dyn. Res. **35**, 123 (2004).
[14] T. Tatsumi and T. Yoshimura, Local similarity of velocity distributions in homogeneous isotropic turbulence, Fluid Dyn. Res. **39**, 221 (2007).
[15] T. Tatsumi, Cross-independence closure for statistical mechanics of fluid turbulence, J. Fluid Mech. **670**, 365 (2011).
[16] A. A. Praskovsky, E. B. Gledzer, M. Y. Karyakin, and A. Y. Zhou, The sweeping decorrelation hypothesis and energy-inertial scale interaction in high Reynolds number flows, J. Fluid Mech. **248**, 493 (1993).
[17] I. Hosokawa, A paradox concerning the refined similarity hypothesis of Kolmogorov for isotropic turbulence, Prog. Theor. Phys. **118**, 169 (2007).
[18] M. Kholmyansky and A. Tsinober, Kolmogorov 4/5 law, nonlocality, and sweeping decorrelation hypothesis, Phys. Fluids **20**, 041704 (2008).
[19] D. Blum, G. Bewley, E. Bodenshatz, M. Gibert, Á. Gylfason, L. Mydlarski, G. Voth, H. Xu, and P. K. Yeung, Signatures of non-universal large scales in conditional structure functions from various turbulent flows, New J. Phys. **13**, 113020 (2011).
[20] M. Germano, The elementary energy transfer between the two-point velocity mean and difference, Phys. Fluids **19**, 085105 (2007).
[21] H. Mouri and A. Hori, Two-point velocity average of turbulence: Statistics and their implications, Phys. Fluids **22**, 115110 (2010).
[22] L. Danaila and L. Mydlarski, Effect of gradient production on scalar fluctuations in decaying grid turbulence, Phys. Rev. E **64**, 016316 (2001).
[23] H. Makita, Realization of a large-scale turbulence field in a small wind-tunnel, Fluid Dyn. Res. **8**, 53 (1991).
[24] L. Mydlarski and Z. Warhaft, On the onset of high-Reynolds-number grid-generated wind tunnel turbulence, J. Fluid Mech. **320**, 331 (1996).
[25] L. Mydlarski, A turbulent quarter century of active grids: From Makita (1991) to the present, Fluid Dyn. Res. **49**, 061401 (2017).
[26] A. Sirivat and Z. Warhaft, The effect of a passive cross-stream temperature gradient on the evolution of temperature variance and heat flux in grid turbulence, J. Fluid Mech. **128**, 323 (1983).
[27] L. Mydlarski, Mixed velocity-passive scalar statistics in high-Reynolds-number turbulence, J. Fluid Mech. **475**, 173 (2003).
[28] J. H. Lienhard and K. N. Helland, An experimental analysis of fluctuating temperature measurements using hot-wires at different overheats, Exp. Fluids **7**, 265 (1989).
[29] A. Berajeklian and L. Mydlarski, Simultaneous velocity-temperature measurements in the heated wake of a cylinder with implications for the modeling of turbulent passive scalars, Phys. Fluids **23**, 055107 (2011).
[30] H. Tennekes and J. L. Lumley, *A First Course in Turbulence* (MIT Press, Cambridge, MA, 1972).
[31] J. Lepore and L. Mydlarski, Effect of the Scalar Injection Mechanism on Passive Scalar Structure Functions in a Turbulent Flow, Phys. Rev. Lett. **103**, 034501 (2009).
[32] M. D. Millionshchikov, On the theory of homogeneous isotropic turbulence, Dokl. Akad. Nauk. SSSR **32**, 611 (1941).
[33] V. M. Gryanik, J. Hartmann, S. Raasch, and M. Schröter, A refinement of the Millionshchikov quasi-normality hypothesis for convective boundary layer turbulence, J. Atmos. Sci. **62**, 2632 (2005).
[34] Z. Warhaft and J. L. Lumley, An experimental study of the decay of temperature fluctuations in grid-generated turbulence, J. Fluid Mech. **88**, 659 (1978).

[35] S. Beaulac and L. Mydlarski, Dependence on the initial conditions of scalar mixing in the turbulent wake of a circular cylinder, Phys. Fluids **16**, 3161 (2004).
[36] G. Xu, Reynolds number dependence of mixed structure functions of temperature and longitudinal velocity, Flow Turbul. Combust. **72**, 369 (2004).
[37] J. Lepore and L. Mydlarski, Finite-Péclet-number effects on the scaling exponents of high-order passive scalar structure functions, J. Fluid Mech. **713**, 453 (2012).
[38] K. R. Sreenivasan and R. A. Antonia, The phenomenology of small-scale turbulence, Annu. Rev. Fluid Mech. **29**, 435 (1997).
[39] A. M. Yaglom, On the local structure of a temperature field in a turbulent flow, Dokl. Akad. Nauk. SSSR **69**, 743 (1949).
[40] R. Hill, Equations relating structure functions of all orders, J. Fluid Mech. **434**, 379 (2001).
[41] L. Danaila, F. Anselmet, T. Zhou, and R. A. Antonia, A generalization of Yaglom's equation which accounts for the large-scale forcing in heated decaying turbulence, J. Fluid Mech. **391**, 359 (1999).